Electromagnetic Excitation of PEC Slotted Cones by Elementary Radial Dipoles – a Semi-Inversion Analysis

Elena K. Semenova, *Member, IEEE*, and Vladimir A. Doroshenko, *Senior Member, IEEE*

Abstract—This paper presents a novel method that is based on the use of the Kontorovich-Lebedev integral transform and the semi-inversion technique, developed for building the efficient and accurate numerical solutions to the boundary-value problems of electromagnetic wave scattering by the 3D coaxial slotted cones. A generic structure under consideration consists of two semi-infinite coaxial circular perfectly electrical conducting (PEC) and zero-thickness cones with periodic longitudinal slots excited by a radial dipole. The considered problem is reduced to an infinite set of linear algebraic equations of the Fredholm second kind that is truncated and solved numerically. A detail analysis of the accuracy and convergence of the method is presented. The basic electromagnetic characteristics such as the field behaviour near the structure singularities, field patterns in the wave zone, and field polarization for various problem parameters are investigated for the cones excited by on-axis elementary dipoles. The slotted cones allow obtaining more directional patterns in wider band than the solid ones.

Index Terms—Coaxial cones, Kontorovich-Lebedev integral transform, semi-inversion method, tip behaviour.

I. Introduction

PEC conical and biconical surfaces belong to canonical geometries in diffraction theory. As for the applications, among the microwave and radiofrequency antennas conical and biconical hollow metallic structures are well known for their wideband properties [1].

The solution of the scalar problem of the acoustic wave scattering by a hard infinite cone was obtained long ago [2]. However, the scattering by conical structures of various geometries still keeps drawing attention of many researchers [3-4]. Various forms of the rigorous field representation in the presence of semi-infinite PEC cones and also the asymptotic solution analyses were considered in [5-11]. Solution representation in the form of series in eigenfunctions [5] is of limited use because of slow convergence of these series in the high-frequency domain. In this sense solution in the form of a contour integral [8] is more convenient and enables one to obtain an expression suitable for numerical analysis in the domain of specular reflection.

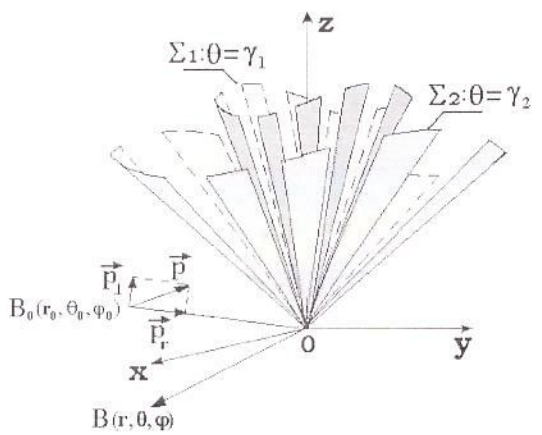

Fig. 1. Problem geometry. Conical structure $\Sigma = \Sigma_1 \cup \Sigma_2$ consists of two semi-infinite PEC circular cones $M_{1,2}$ each with N longitudinal periodical slots $S_{1,2}$, having common vertex O and axis OZ. A radial dipole source is at B_0.

In the case of diffraction by a semi-infinite elliptic cone it is possible to separate variables in sphero-conical coordinate system [12-13]. Diffraction by cones of arbitrary cross section has been a challenge in diffraction theory for many years [4, 14]. The approach developed in [4, 14] allows to obtain a solution in the high-frequency case, but it is not valid for the investigation of the field in the near zone and at the cone tip.

Numerous papers have been devoted to the investigation of diffraction by finite cones. The Kirchhoff method or physical optics (PO) was applied in [15] where the main contribution of a finite cone to the axially scattered field was found. Later the method of geometrical theory of diffraction (GTD) and more universal method of the physical theory of diffraction (PTD) were applied for solving the diffraction problems for finite circular and elliptic cones [16-18]. However the solutions obtained by such heuristic methods fail to determine the field and current near the tip of the cone and require verification by the accurate methods [19-20].

Studying the field behaviour near the singularities of a scatterer is one of the principal tasks in the rigorous diffraction

Manuscript received 9 August, 2007. Revised 25 March, 2008.

The authors are with the Mathematics Department, Kharkiv National University of Radio Electronics, Kharkiv 61166, Ukraine (e-mail: h_semenova@yahoo.com).

This work was partially supported by the Ministry of Education and Science, Ukraine.

theory. Various types of structures with singular points are widely used in the waveguide and antenna systems. Knowledge of the field behaviour near such points and edges allows estimates of the accuracy of the numerical solutions and speeding up the algorithm convergence. Works [21-23] were devoted to studying the field behaviour near the tip of a PEC solid cone of arbitrary cross-section (in particular, a plane angular sector).

Open conical and biconical structures find applications, for example, in radar where reflectors with the necessary beam forming properties can be developed. Besides, it is known that for the radiation of powerful super-wideband impulses the radiation pattern (RP) of an element of a scanning antenna grating should be close to the cardioid pattern.

Antenna built on the basis of a solid cone or bicone can be super-wideband however fail to produce directive RPs. The use of additional reflector for obtaining a cardioid RP sharply worsens impedance characteristics of a conical structure and increases its size. A remedy can be a replacement of the full metallic conical surface by its part. This motivates research into electromagnetic wave diffraction problems for more complicated open conical structures.

Active development in the area of electromagnetic antennas design and measurements requires accurate and efficient numerical algorithms of computer modelling of wave propagation and scattering. For the 3D wave diffraction problems associated with complicated conical radiating structures this is a tedious task for the finite-difference, beam propagation, finite element or transmission line methods. The use of semi-analytical techniques promises a great advantage especially when multiple calculations are needed in the computer-aided design. Therefore the importance of the development of a mathematical approach that guarantees fast convergence and controlled accuracy when applied to conical structures with slots is evident.

An accurate approach to solving the problem of electromagnetic wave diffraction by a PEC infinite cone was proposed in [24]. It is based on the Kontorovich-Lebedev integral transform, which allows studying 2D and 3D problems with complicated open conical geometries [25]. This approach was applied to a single infinite PEC cone with longitudinal slots in [26]. The analytical solutions in some special cases such as "semi-transparent" cone (i.e., with large number of slots ($N >> 1$) much narrower than the period) and cones with narrow slots or strips were obtained. However, no numerical analysis for arbitrary slot size was performed.

In view of these circumstances, the development and application of an accurate analytical-numerical approach for solving the problems with 3D PEC open conical and biconical slotted structures for a wide range of angular parameters are of great interest. We are going to build this approach using the semi-inversion technique.

This paper is organized as follows. The problem geometry and solution method for the radial dipole source are presented in Section II. The dual series equations are converted to a Fredholm second-kind infinite matrix equation by the semi-inversion technique in Section III. Special attention is paid in Section IV to the regions close to the structure tip and slot edges, where the field exhibits singular behaviour. Sections V and VI present some numerical characteristics for the scattered field that show its polarisation and far-field patterns. Conclusions are given in Section VII.

II. Problem Formulation

A 3-D double-cone structure presented in Fig.1 is considered in the spherical coordinates (r,θ,φ) with the origin at the common tip of the cones. A time-harmonic ($\sim \exp(i\omega t)$) radial dipole with the moment $\vec{p}_s = p_0^{(s)}\vec{r}_0$ ($s=1$ is for the electric dipole, $s=2$ is for the magnetic one) is located at the point B_0. The cone surfaces Σ_j are defined by the equations $\theta=\gamma_j$, $j=1,2$. Each surface has zero thickness and N slots of the angular width d_1 (for cone Σ_1) and of the angular width d_2 (for cone Σ_2), cut with the same angular period $l=2\pi/N$. The orientation of the slots on inner cone relative to those in the outer is arbitrary.

Denote the PEC strips of the cone Σ_j as M_j and the slots as S_j. The vectors $\vec{E}$ and $\vec{H}$ of the total field must satisfy the Maxwell equations, boundary condition on the PEC strips: $\vec{E}_{\tau}\big|_M = 0$, ($M = M_1 \bigcup M_2$), the condition of local energy finiteness and the radiation condition at infinity.

The conditions mentioned above guarantee the uniqueness of solution [27]. In order to find it, it is convenient to use the auxiliary function, Debye potential $\upsilon^{(s)}$, which satisfies 3D homogeneous Helmholtz equation, $\Delta\upsilon^{(s)}+k^2\upsilon^{(s)}=0$ (k is the wavenumber) outside the cone strips and the source; boundary condition on the strips, $\partial^{s-1}\upsilon^{(s)}/\partial n^{s-1}\big|_M = 0$, where $s=1$ for the Dirichlet condition, and $s=2$ for the Neumann condition; the condition of radiation, and the condition of local energy finiteness. Note that it using only one Debye potential (either $\upsilon^{(1)}$ or $\upsilon^{(2)}$) is enough to solve the problem with a radial-dipole excitation. In the case of source being arbitrarily oriented dipole or plane-wave excitation one needs their combination to build the solution.

Decomposing the total field into incident and scattered fields, $\vec{E}=\vec{E}^{0}+\vec{E}^{sc}$, $\vec{H}=\vec{H}^{0}+\vec{H}^{sc}$, we represent $\upsilon^{(s)}$ as

$$\upsilon^{(s)} = \upsilon_0^{(s)} + \upsilon_{sc}^{(s)}, \quad s=1,2, \quad \upsilon_0^{(s)} = \frac{p_0^{(s)}}{r_0}\frac{e^{-qR}}{4\pi R} \qquad (1)$$

where $\upsilon_0^{(s)}$ and $\upsilon_{sc}^{(s)}$ correspond to the dipole field and the field scattered by the conical structure, respectively.

To find the solution we apply the Kontorovich-Lebedev integral transform [24]:

$$\upsilon_{sc}^{(s)} = -\frac{1}{2}\int_0^{\infty} \tau \sinh(\pi\tau) e^{\pi\tau} \hat{\upsilon}_{sc}^{(s)} \frac{H_{i\tau}^{(2)}(kr)}{\sqrt{r}} d\tau$$
$$\hat{\upsilon}_{sc}^{(s)} = \int_0^{\infty} \upsilon_{sc}^{(s)} \frac{H_{i\tau}^{(2)}(kr)}{\sqrt{r}} dr \qquad (2)$$

and expand the unknown spectral density function as follows:

$$\hat{\upsilon}_{sc}^{(s)} = -\sum_{m=-\infty}^{+\infty} a_{m\tau}^{(s)} b_{i\tau}^{(s),p}(\theta_0) U_{m\tau}^{(s)}(\theta,\varphi) \qquad (3)$$

where $H_{i\tau}^{(2)}(kr)$ is the Hankel function of the second kind, coefficients $a_{m\tau}^{(s)}$ and $b_{i\tau}^{(s),p}(\theta_0)$ are given in Appendix A, $U_{m\tau}^{(s)}(\theta,\varphi)$ is unknown function. The radial dipole can be located inside the cone Σ_1 ($\theta_0 < \gamma_1$, $p=1$) or outside the cone Σ_2 ($\theta_0 > \gamma_2$, $p=2$).

The boundary condition imposed on the strips and the field continuity condition on the slots yield, together with (3), the dual series equations (DSEs) for the unknown coefficients $z_{m,n}^{(s),j}$ connected with the expansion coefficients of $U_{m\tau}^{(s)}(\theta,\varphi)$ by the expressions given in Appendices A and B:

$$\sum_{n=-\infty}^{+\infty} z_{m,n}^{(s),j} e^{i(n+\nu)N\varphi} = \hat{g}_{i\tau}^{(s),p}(\gamma_j) e^{i(m_0+\nu)N\varphi},\ \varphi \in M_j,\ j=1,2 \quad (4)$$

$$\sum_{n=-\infty}^{+\infty} \left[N(n+\nu)\right]^{\tilde{\delta}(s)} \frac{|n|}{n} (1-\varepsilon_{m,n,j}^{(s)}) \cdot \left\{ z_{m,n}^{(s),j} \left[\hat{h}_{i\tau}^{(s),1(n+\nu)N}(\pi-\gamma_2,\pi-\gamma_1) \right]^{j-1} - z_{m,n}^{(s),2} \left[\hat{h}_{i\tau}^{(s),1(n+\nu)N}(\gamma_1,\gamma_2) \right]^{2-j} \right\} \cdot e^{i(n+\nu)N\varphi} = 0,\ \varphi \in S_j,\ j=1,2 \qquad (5)$$

$$M_j = \left\{ \theta = \gamma_j, \frac{\pi d_j}{l} < |N\varphi| \le \pi \right\},\ S_j = \left\{ \theta = \gamma_j, |N\varphi| \le \frac{\pi d_j}{l} \right\}.$$

Coefficients $\hat{g}_{i\tau}^{(s),p}(\gamma_j)$, $\hat{h}_{i\tau}^{(s),1(n+\nu)N}$, $\varepsilon_{m,n,j}^{(s)}$ are given in Appendix B. Note that $\varepsilon_{m,n,j}^{(s)}$ behave as

$$\varepsilon_{m,n,j}^{(s)} = O\left(\frac{1}{(n+\nu)^2 N^2}\right),\ nN >> 1. \qquad (6)$$

where $m/N = m_0 + \nu$, m_0 is the integer nearest to m/N, $-1/2 \le \nu < 1/2$, and $\delta(s) = (-1)^{s-1}$.

In particular case when the cone Σ_1 is absent, i.e. $\Sigma = \Sigma_2$, DSEs (4), (5) can be reduced to (omitting index j):

$$\sum_{n=-\infty}^{+\infty} x_{m,n}^{(s)} e^{inN\varphi} = e^{im_0 N\varphi},\quad \varphi \in M \qquad (7)$$

$$\sum_{n=-\infty}^{+\infty} \left[N(n+\nu)\right]^{\tilde{\delta}(s)} \frac{|n|}{n} (1-\varepsilon_{m,n}^{(s)}) x_{m,n}^{(s)} e^{inN\varphi} = 0,\quad \varphi \in S \qquad (8)$$

If the cone Σ_2 has slots and Σ_1 has not, DSEs (4), (5) can be written as:

$$\sum_{n=-\infty}^{+\infty} x_{m,n}^{(s)} e^{inN\varphi} = e^{im_0 N\varphi},\quad \varphi \in M_j,\ j=1,2 \qquad (9)$$

$$\sum_{n=-\infty}^{+\infty} \left[N(n+\nu)\right]^{\tilde{\delta}(s)} \frac{|n|}{n} (1-\varepsilon_{m,n,2}^{(s)}) x_{m,n}^{(s)} e^{inN\varphi} = \left[N(m_0+\nu)\right]^{\tilde{\delta}(s)} \frac{|m_0|}{m_0} (1-\varepsilon_{m,m_0,2}^{(s)}) \cdot C \cdot e^{im_0 N\varphi},\ \varphi \in S_2 \qquad (10)$$

III. Fredholm Matrix Equation of the Second Kind

Each pair of the obtained DSEs (4)-(5), (7)-(8), and (9)-(10) is the first-kind equation. By using the semi-inversion technique (for a review of such techniques in computational electromagnetics see [28]) based on analytical solution to the Riemann-Hilbert problem [29], these DSEs are reduced to the Fredholm infinite matrix equations of the second kind that can be efficiently solved numerically.

For example, for the radial electric dipole ($s=1$) DSEs (7)-(8) are reduced to the following matrix equation:

$$y_{m,0}^{(1)} - \frac{\nu\left(P_\nu(-u_1) + P_{\nu-1}(-u_1)\right)}{2P_{\nu-1}(-u_1)} \sum_{p=-\infty}^{\infty} \frac{|p|}{p} \delta_{m,p}^{(1)} V^p(u_1) y_{m,p}^{(1)} = V^{m_0}(u_1), \qquad (11)$$

$$y_{m,n}^{(1)} - y_{m,0}^{(1)} P_n(u_1) - \sum_{p=-\infty}^{\infty} \frac{|p|}{p} \delta_{m,p}^{(1)} V_{n-1}^{p-1}(u_1) y_{m,p}^{(1)} = V_{n-1}^{m_0-1}(u_1),\ n \ne 0 \qquad (12)$$

where

$$y_{m,n}^{(1)} = (-1)^{n-m_0} \cdot \frac{n+\nu}{m_0+\nu} \cdot \frac{|n|}{n} \left(1-\varepsilon_{m,n}^{(1)}\right) x_{m,n}^{(1)}, \qquad (13)$$

$$1-\delta_{m,n}^{(1)} = \left[1-\varepsilon_{m,n}^{(1)}\right]^{-1}, \qquad (14)$$

coefficients $V^{m_0}(u_1)$, $V_{n-1}^{m-1}(u_1)$ are presented in Appendix C, $P_n(u_1)$ is the Legendre polynomial, $u_1 = \cos\left[\pi(l-d)/l\right]$.

This set of equations can be written in operator notation as:

$$Y + AY = B, \qquad (15)$$

where

$$Y = \left\{y_{m,n}\right\}_{n=-\infty}^{+\infty},\ A = \left\{a_{p,n}^m\right\}_{p,n=-\infty}^{+\infty},\ B = \left\{b_{m,n}\right\}_{n=-\infty}^{+\infty} \qquad (16)$$

and the elements of $a_{p,n}^m$ and $b_{m,n}$ are defined by (11) and (12). The most important feature of (15) is that $\|A\|_{l_2} < \infty$ and $\|B\|_{l_2} < \infty$ (provided that the dipole is located off Σ). Then (15) is a Fredholm second kind operator equation.

The set (9), (10) can be reduced to a similar matrix equation. Note that the coefficients $x_{m,n}^{(s)}$ do not depend on the wavenumber that is convenient for finding the field both near the vertex ($kr << 1$) and far from it ($kr >> 1$). The solution convergence is guaranteed by the Fredholm nature of (15), in the sense that more accurate numerical solutions are obtained

by solving finite matrix equations truncated to progressively larger orders.

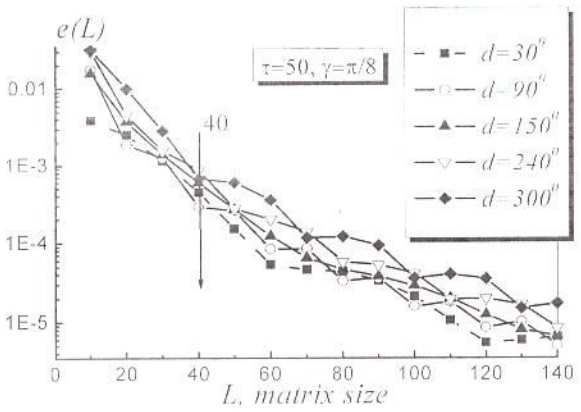

Fig. 2. The relative error versus the truncation order of the matrix (15).

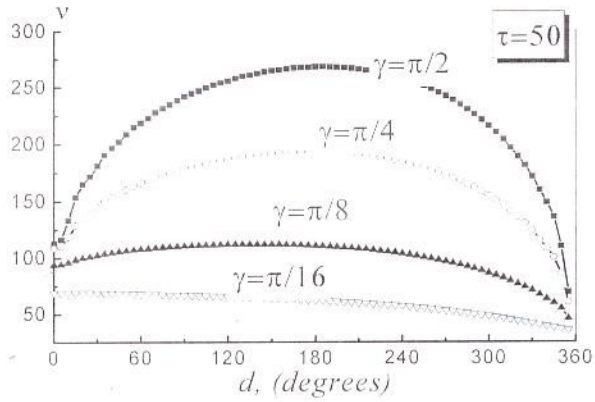

Fig. 3. Condition number of the matrix equation (15) vs. the slot width. The source is on the cone axis, $\theta_0 = \pi$, and cone Σ_1 has one

The rate of convergence can be estimated through the calculation of the relative error of truncation [28]:

$$e(L) = \frac{\| X_L - X_{L+1} \|_{l_2}}{\| X_L \|_{l_2}}, \quad X_L = \{x_n^{(L)}\}, \tag{17}$$

where L is the order of truncation. The plots presented in Fig. 2 show that taking only 40 equations is enough to obtain the solution with relative error $e(L) \le 10^{-3}$ for a cone with arbitrary slot width.

The condition number of the matrix is another important quantity because the smaller this number, the better the stability of numerical solution. The condition number of the matrix (15) is calculated as $\nu = \| I + A \| \cdot \| (I + A)^{-1} \|$, where I is the identity operator, and depicted in Fig. 3. As the value of ν does not exceed a few hundred, the obtained equations are well-conditioned.

IV. Field Near the Structure Singularities

The analysis of the field behaviour near the structure singularities, such as the cone tip or slot edges, is one of the key problems in the rigorous wave diffraction theory. The knowledge of the field behaviour is important for building the efficient computational codes for 3-D structures of more general shapes. We have studied the field behaviour (i) near the tip of the cone $\Sigma = \Sigma_2$ with one slot (cone Σ_1 is absent) (Figs. 4 and 5) and (ii) near the common tip of two coaxial cones, $\Sigma = \Sigma_1 \bigcup \Sigma_2$, where cone Σ_1 has no slots and cone Σ_2 has only one slot (Figs. 6 and 7). As a source, we consider a radial electrical dipole ($s = 1$) on the cone axis ($\theta_0 = \pi$).

The field components near the conical tip behave as

$$| \vec{E} | \sim | kr |^{-1+\alpha}, \; | \vec{H} | \sim | kr |^{\alpha}, \; kr \ll 1 \tag{18}$$

where $\alpha = -1/2 + \min_n \hat{\mu}_n$, and $\hat{\mu}_n$ are the eigenvalues of Debye potential $\upsilon^{(1)}$ (see Appendix D).

Fig. 5 gives the dependence of the electrical field singularity degree, α, on the conical angle γ for several values of the slot width d^0, for the structure (i). There is also a curve for the solid cone that is shown to demonstrate the slot effect. It is obvious that with the appearance of a slot the degree of electrical field singularity increases. Magnetic field has no field singularity near the cone tip.

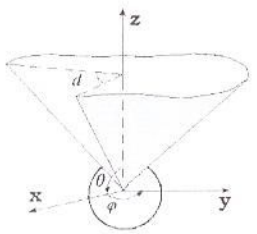

Fig. 4. Near-field region in the case (I).

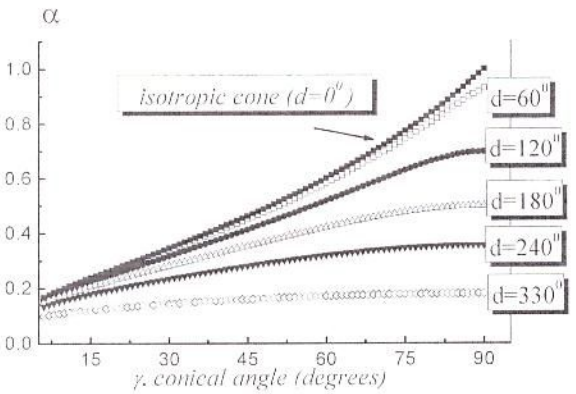

Fig. 5. Field singularity α in the case (I) for different slot widths.

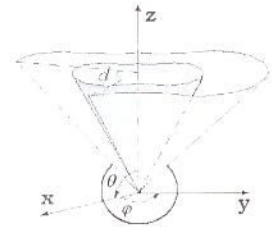

Fig. 6. Near-field region in the case (II).

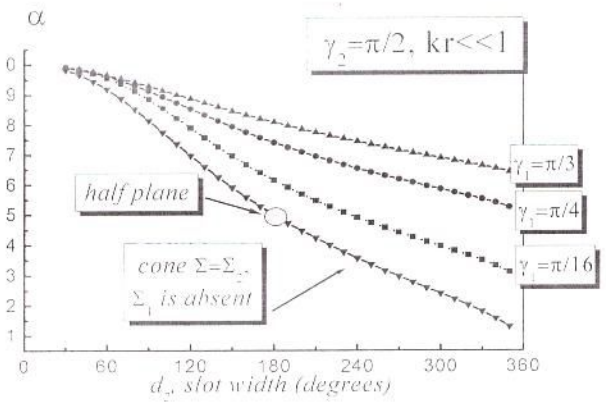

Fig. 7. Field singularity α in the case (II) for different angles γ_1 of the solid cone.

The behavior of the electrical field singularity value in the case (ii) is presented in Fig.7 as dependences of α on the slot width d^0 for several values of the solid cone angle γ_1. It can be seen that increasing the angle γ_1 leads to decreasing the singularity of the electrical field near the tip.

If $d_2 = 180^0$, the plane with a cut turns to the half-plane and the singularities of E и H fields turn to the known square-root singularities, $|kr|^{-1/2}$, near the edge [23]. This fact is the evidence of the correctness of the obtained results.

V. Polarization of the Scattered Field

To analyze the polarization of the scattered field it is convenient to introduce the polarization characteristic, $Y(\theta,\varphi) = E_\theta / E_\varphi$, in the form:

$$Y(\theta,\varphi) = |Y(\theta,\varphi)|\, e^{iArgY(\theta,\varphi)} \qquad (19)$$

As known, the values $ArgY(\theta,\varphi) = \pm\pi/2$ correspond to the circular polarization of the field, and $ArgY(\theta,\varphi) = 0,\pm\pi$ are for the linear polarization. The rest of the argument values correspond to the elliptic polarization. Note that if $|Y(\theta,\varphi)| \to 0$ or $|Y(\theta,\varphi)| \to \infty$, polarization becomes linear.

It is known that the polarization of the field scattered by a solid PEC cone is linear if the source is placed on the cone axis. According to the obtained results (Figs. 8, 9), we can conclude that the field scattered by the cone with one slot has an elliptic polarization. Only for a narrow slot ($d < 10^0$) or a narrow strip ($d > 300^0$) does the polarization of the scattered field transform to linear.

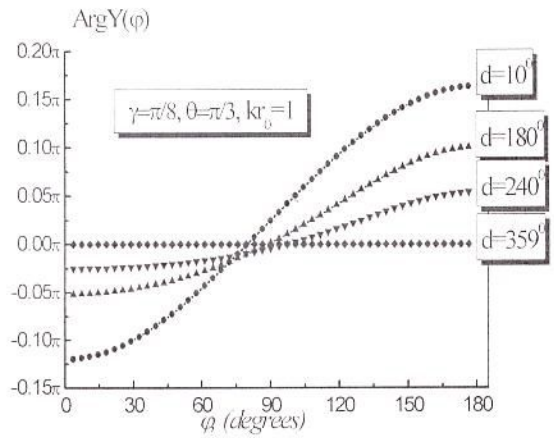

Fig. 8. Argument of the polarization characteristic for one cone with one slot as a function of the azimuth coordinate φ.

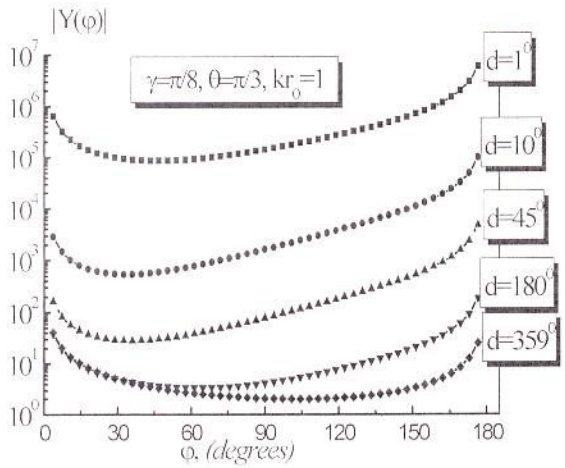

Fig. 9. Absolute value of the polarization characteristic for one cone with one slot, as a function of the azimuth coordinate φ.

VI. Field in the Wave Zone

Consider the far zone where the diffracted field is an outgoing spherical wave. The diffracted field can be presented as the sum of an image field reflected from the cone surface and the field caused by presence of the tip. There is no field of specular reflection in the domain of the space defined by the inequality $2\gamma_2 < \theta$, that is why here the diffracted field is characterized only by the field scattered from the common tip of the double-cone surface Σ. The numerical solution of the matrix equation (15) and the use of an asymptotic form ($kr >> 1$) for the potential (2) allow studying numerically the diffracted field pattern in the wave zone. Suppose that the source is at the cone axis, i.e. $\varphi_0 = 0$, $\theta_0 = \pi$, and $m = 0$.

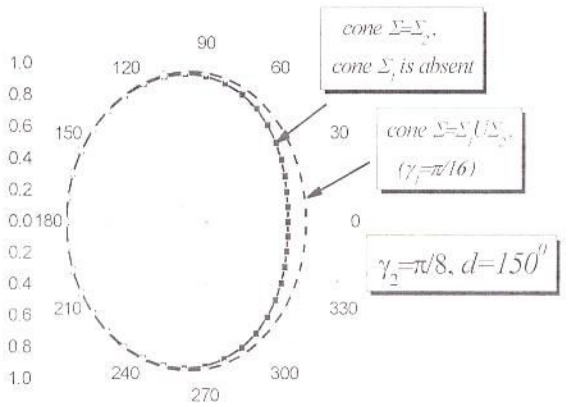

Fig. 10. Scattered field in the wave zone for one cone, $\Sigma=\Sigma_2$, and for two coaxial cones $\Sigma=\Sigma_1\cup\Sigma_2$, where Σ_1 is a full cone with $\gamma_1=\pi/16$, and Σ_2 is a cone with $\gamma_2=\pi/8$ and one slot, $d=150^0$. The source is a radial electrical dipole.

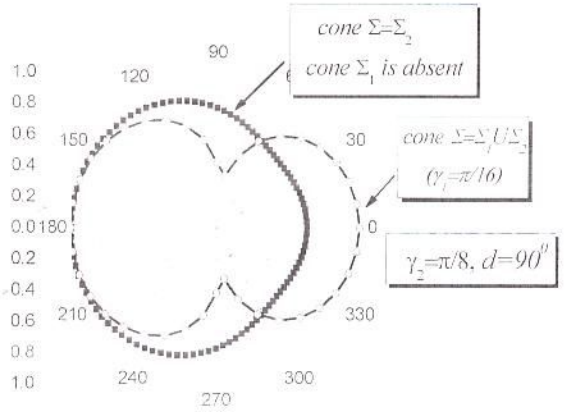

Fig. 11. The same as in Fig. 10, however for $d=90^0$ and a radial magnetic dipole as a source.

Fig. 10 depicts the scattered E-field patterns for one PEC cone with one slot ($N=1$) and two PEC coaxial cones excited by the radial electrical dipole. For the magnetic dipole case, see Fig. 11. The patterns are symmetrical with respect to the slot center ($\varphi=0^0$). Analysis shows that their shape can be controlled by the change of the slot width d^0 and cone angles $\gamma_{1,2}$. One can see that the presence of the solid cone Σ_1 effects the scattered field in small manner in the case of excitation with a radial electrical dipole (Fig. 10). However, if the source is a radial magnetic dipole (Fig. 11), the solid cone has more significant influence on the scattered field.

VII. Conclusions

The PEC coaxial slotted cones excited by elementary radial dipoles have been considered. The proposed solution method is based on applying the Kontorovich-Lebedev integral transform and the semi-inversion technique. Each problem has been reduced to solving an infinite Fredholm second kind equation with a well-conditioned matrix. This can be done numerically to any pre-specified accuracy (within machine precision) after matrix truncation.

Numerical results for the field singularity in the vicinity of the PEC slotted cone tip have been presented. This may be used to improve the convergence of numerical solutions for many other practical problems, by introducing the singularity as *a priori* information. Our results, in particular, allow finding the field behaviour near the tip of a cone with longitudinal slots that can be used in the electromagnetic diagnostics of cracks on a conical surface.

We have also analyzed the effects accompanying electromagnetic wave diffraction by the structure consisting of two coaxial PEC circular cones with longitudinal slots. They have shown that the shape of the far-field pattern can be controlled by the change of the slot width and cone angles. One can see that the presence of a solid cone Σ_1 has significant influence on the shape of the pattern in the case of the radial magnetic dipole as a source, in contrast to the radial electric dipole. Also, by varying the slot width one can change the shape of the scattered field pattern considerably.

Appendix A

Coefficients for the unknown function (3) are as follows:

$$a_{m\tau}^{(s)}=-\frac{p_0^{(s)}\pi}{r_0\cosh\pi\tau}\frac{H_{i\tau}^{(2)}(kr_0)}{\sqrt{r_0}}(-1)^m e^{-im\varphi_0}\frac{\Gamma(1/2-m+i\tau)}{\Gamma(1/2+m+i\tau)}, \quad (20)$$

$$b_{i\tau}^{(s),p}(\theta_0)=\frac{d}{d\gamma_p}F(\gamma_p,\theta_0,m,\tau)\chi\left((-1)^p(\theta_0-\gamma_p)\right), \quad (21)$$

where $F(\theta,\theta_0,m,\tau)=\begin{cases}P_{-1/2}^m(\cos\theta)P_{-1/2}^m(-\cos\theta_0),\theta<\theta_0\\P_{-1/2}^m(-\cos\theta)P_{-1/2}^m(\cos\theta_0),\theta_0<\theta\end{cases}$,

$P_{-1/2+i\tau}^m(x)$ is the associated Legendre function and $\chi(a)$ is the Heaviside function, i.e. 1 if $a\ge 0$ or 0 otherwise.

The unknown function $U_{m\tau}^{(s)}$ can be presented in the form of the following series in separate regions:

$$U_{m\tau}^{(s)}=\begin{cases}\sum_{n=-\infty}^{+\infty}\alpha_{mn}^{(s)}P_{-1/2+i\tau}^{m+nN}(\cos\theta)e^{i(m+nN)\varphi}, 0<\theta<\gamma_1\\ \sum_{n=-\infty}^{+\infty}\left[\beta_{mn}^{(s)}P_{-1/2+i\tau}^{m+nN}(\cos\theta)+\xi_{mn}^{(s)}P_{-1/2+i\tau}^{m+nN}(-\cos\theta)\right]\\ \qquad\cdot e^{i(m-nN)\varphi} \quad \gamma_1<\theta<\gamma_2\\ \sum_{n=-\infty}^{+\infty}\eta_{mn}^{(s)}P_{-1/2+i\tau}^{m+nN}(-\cos\theta)e^{i(m+nN)\varphi}, \gamma_2<\theta<\pi;\end{cases} \quad (22)$$

The links between the unknown coefficients $\alpha_{mn}^{(s)}$, $\beta_{mn}^{(s)}$, $\xi_{mn}^{(s)}$, $\eta_{mn}^{(s)}$ are determined due to the boundary conditions on the

surfaces $\theta=\gamma_1$, $\theta=\gamma_2$, therefore coefficients $\beta_{mn}^{(s)}$ and $\xi_{mn}^{(s)}$ can be expressed through $\alpha_{mn}^{(s)}$ and $\eta_{mn}^{(s)}$ as

$$\beta_{mn}^{(s)}=-\frac{\left[\alpha_{mn}^{(s)}\frac{d^{s-1}}{d\gamma_1^{s-1}}P_{-1/2+i\tau}^{m+nN}(\cos\gamma_1)-\eta_{mn}^{(s)}\frac{d^{s-1}}{d\gamma_1^{s-1}}P_{-1/2+i\tau}^{m-nN}(-\cos\gamma_1)\right]}{C^{-1}\cdot(1-C)\frac{d^{s-1}}{d\gamma_1^{s-1}}P_{-1/2+i\tau}^{m+nN}(\cos\gamma_1)} \tag{23}$$

$$\xi_{mn}^{(s)}=-\frac{\left[\alpha_{mn}^{(s)}\frac{d^{s-1}}{d\gamma_2^{s-1}}P_{-1/2+i\tau}^{m+nN}(\cos\gamma_2)-\eta_{mn}^{(s)}\frac{d^{s-1}}{d\gamma_2^{s-1}}P_{-1/2+i\tau}^{m+nN}(-\cos\gamma_2)\right]}{C^{-1}\cdot(1-C)\cdot\frac{d^{s-1}}{d\gamma_2^{s-1}}P_{-1/2+i\tau}^{m+nN}(-\cos\gamma_2)} \tag{24}$$

where

$$C=\frac{\frac{d^{s-1}}{d\gamma_1^{s-1}}P_{-1/2+i\tau}^{m+nN}(\cos\gamma_1)\frac{d^{s-1}}{d\gamma_2^{s-1}}P_{-1/2-i\tau}^{m+nN}(-\cos\gamma_2)}{\frac{d^{s-1}}{d\gamma_1^{s-1}}P_{-1/2+i\tau}^{m+nN}(-\cos\gamma_1)\frac{d^{s-1}}{d\gamma_2^{s-1}}P_{-1/2+i\tau}^{m+nN}(\cos\gamma_2)}. \tag{25}$$

APPENDIX B

Unknown coefficients in DSEs (4)-(5) have the form as

$$z_{m,n}^{(s),j}=\left[x_{m,n}^{(s)}\right]^{2-j}+\left[y_{m,n}^{(s)}\right]^{j-1}, \tag{26}$$

where $j=1,2$ and

$$x_{m,n-m_0}^{(s)}=\alpha_{mn}^{(s)}\frac{d^{s-1}}{d\gamma_1^{s-1}}P_{-1/2-i\tau}^{(n+\nu)N}(\cos\gamma_1), \tag{27}$$

$$y_{m,n-m_0}^{(s)}=\eta_{mn}^{(s)}\frac{d^{s-1}}{d\gamma_2^{s-1}}P_{-1/2+i\tau}^{(n+\nu)N}(\cos\gamma_2) \tag{28}$$

Coefficients $\hat{g}_{i\tau}^{(s),p}(\gamma_j)$, $\hat{h}_{i\tau}^{(s)(n+\nu)N}$, $\varepsilon_{m,n,i}^{(s)}$ in DSEs (4)-(5) are given by formulas

$$\hat{g}_{i\tau}^{(s),p}(\theta,\theta_0,m)\equiv\hat{g}_{i\tau}^{(s),p}(\theta)=\frac{1}{\hat{b}_{i\tau}^{(s),p}}\frac{d^{s-1}}{d\theta^{s-1}}F(\theta,\theta_0,m,\tau), \tag{29}$$

$$\hat{h}_{i\tau}^{(s)(n-\nu)N}=\frac{d^{s-1}}{dx^{s-1}}P_{-1/2+i\tau}^{(n-\nu)N}(\cos x)\left[\frac{d^{s-1}}{dy^{s-1}}P_{-1/2-i\tau}^{(n-\nu)N}(\cos y)\right]^{-1}, \tag{30}$$

$$\left[N(n+\nu)\right]^{\delta(s)}\frac{|n|}{n}(1-\varepsilon_{m,n,i}^{(s)})=\frac{(-1)^{(n-\nu)N-s-1}ch\pi\tau}{\pi(\sin\gamma_j)^{1-\delta(s)}}$$

$$\cdot\frac{\Gamma(\frac{1}{2}+i\tau+(n+\nu)N)}{\Gamma(\frac{1}{2}+i\tau-(n+\nu)N)}\frac{(1-C)^{-1}}{\frac{d^{s-1}}{d\gamma_j^{s-1}}P_{-1/2-i\tau}^{(n-\nu)N}(\cos\gamma_j)\frac{d^{s-1}}{d\gamma_j^{s-1}}P_{-1/2-i\tau}^{(n-\nu)N}(-\cos\gamma_j)} \tag{31}$$

APPENDIX C

According to [29], coefficients $V^{m_0}(u_1)$, $V_{n-1}^{m-1}(u_1)$ in the matrix equation (11),(12) are given by

$$V_{n-1}^{m-1}(u)=\begin{cases}\frac{1}{2}\sum_{p=0}^{m}\rho_{m-p}(u)P_{p-n}(u), & m\geq 1\\ \frac{1}{2}[P_{-n}(u)-P_n(u)], & m=0\\ -\frac{1}{2}\sum_{p=0}^{-m}\rho_{-m-p}(u)P_{p-n}(u), & m\leq 0\end{cases} \tag{32}$$

where

$\rho_0=1$, $\rho_1(u)=-u$, $\rho_{n\geq 2}(u)=P_n(u)-2uP_{n-1}(u)+P_{n-2}(u)$, and

$$\Gamma^{nn}(u)=\frac{1}{n+\nu}\{P_n(u)-\frac{P_{\nu-1}(-u)}{P_\nu(-u)+P_{\nu-1}(-u)}[P_n(u)-P_{n-1}(u)]\}. \tag{33}$$

A shorter form of the matrix elements can be obtained after joining (11) and (12) in one equation: for details see [30].

APPENDIX D

To find the eigenvalues, substitute the Debye potential $\upsilon_{sc}^{(1)}$ (2) into the formulas for the field components:

$$E_r=\left(\frac{\partial^2}{\partial r^2}-q\frac{\partial^2}{\partial t^2}\right)\cdot\left(r\upsilon^{(1)}\right),\quad H_r=0$$

$$E_\theta=\frac{1}{r}\frac{\partial^2}{\partial r\partial\theta}\left(r\upsilon^{(1)}\right),\qquad H_\upsilon=\frac{q}{w}\frac{1}{\sin\theta}\frac{\partial}{\partial\varphi}\upsilon^{(1)} \tag{34}$$

$$E_\varphi=\frac{1}{r\sin\theta}\frac{\partial^2}{\partial r\partial\varphi}\left(r\upsilon^{(1)}\right),\qquad H_\varphi=-\frac{q}{w}\frac{\partial}{\partial\theta}\upsilon^{(1)}$$

Then, after integrating along the imaginary axis ($\tilde{\mu}=i\tau$, $0\leq\tau<+\infty$) and closing the integration contour in the right half plane ($\mathrm{Re}\,\tilde{\mu}>0$), one can obtain the field representation in the form of series in residuals.

In this case, the spectrum of the boundary-value problem (i.e. the set of eigenvalues) coincides with the poles of coefficients $x_n^{(1)}$. To find the poles we use the Cramer rule:

$$x_n^{(1)}=\frac{\Delta_{\tilde{\mu},n}^{(1)}}{\Delta_{\tilde{\mu}}^{(1)}}, \tag{35}$$

where $\Delta_{i\tau}^{(1)}$ is the determinant of the matrix (11)-(12). Thus, finding the spectrum is equivalent to finding the roots of equation

$$\Delta_{\tilde{\mu}}^{(1)}(d,\gamma,N)=0. \tag{36}$$

The distinctive feature of this problem is that the spectral parameter can be any of the angular values γ_j and d; it is also a function of the number of strips N. The spectrum is discrete and defines the natural modes, which may exist in the

given structure. The smallest eigenvalues determines the field behavior near the tip of the open cone (see [21] for details).

ACKNOWLEDGMENT

The authors are grateful to Dr. N. Sakhnenko for many useful discussions and to anonymous reviewers for valuable comments and advices.

REFERENCES

[1] J. D. Kraus, R. J. Marhefka, *Antennas*, McGraw-Hill, 2nd Ed., 1988.

[2] H. S. Carslaw, "The scattering of sound waves by a cone", *Math. Ann.*, vol. 75, no.1, pp. 133-147, March 1914.

[3] J. M. L. Bernard, M. A. Lyalinov, "Spectral domain solution and asymptotics for the diffraction by an impedance cone," *IEEE Trans. Antennas Propag.*, vol. 49, no. 12, pp. 1633-1637, Dec. 2001.

[4] V. M. Babich, V. P. Smyshlyaev, D. B. Dementyev, B. A. Samokhin, "Numerical calculation of the diffraction coefficients for an arbitrary shaped perfectly conducting cone," *IEEE Trans. Antennas Propag.*, vol. 44, no. 5, pp. 740-747, May 1996.

[5] L. L. Bailin, S. Silver, "Exterior electromagnetic boundary value problems for spheres and cones," *IRE Trans. Antennas Propag.*, vol. 4, no. 1, pp. 5-16, Jan. 1956.

[6] L. B. Felsen, "Plane wave scattering by small angle cone," *IRE Trans. Antennas Propag.*, vol. 5, pp.121-129, Jan. 1957.

[7] L. B. Felsen, "Asymptotic expansion of the diffracted wave for a semi-infinite cone," *IRE Trans. Antennas Propag.*, vol. 5, no. 4, pp. 402-404, Oct. 1957.

[8] L. B. Felsen, "Radiation from ring sources in the presence of a semi-infinite cone," *IRE Trans. Antennas Propag.*, vol. 7, no. 2, pp. 168-180, Apr. 1959.

[9] K. M. Siegel, J. W. Crispin, C. E. Schensted, "Electromagnetic and acoustical scattering from a semi-infinite cone," *J. Appl. Phys.*, vol. 26, pp. 309-313, March 1955.

[10] J. J. Bowman, T. B. A. Senior, P. L. E. Uslenghi, *Electromagnetic and Acoustic Scattering by Simple Shapes*, North Holland, Amsterdam, Hemisphere Publ., 1969.

[11] R. C. Spencer, *Backscattering from Conducting Surfaces*, Air Force Cambridge Res. Labs., Cambridge, Mas., Rept. CRL-E5070, Apr. 1951.

[12] L. Kraus, L. M. Levine, "Diffraction by an elliptic cone," *Comm. Pure Appl. Mathematics*, vol. 14, pp. 49-68, 1961.

[13] E. Vafiadis, J. N. Sahalos, "Analysis of semi-infinite elliptic conical scattered," *J. Phys. D*, vol. 18, pp. 1475-1493, 1985.

[14] V. P. Smyshlyaev, "The high-frequency diffraction of electromagnetic waves by cones of arbitrary cross-section," *SIAM J. Appl. Mathemat.*, vol. 53, pp. 670-688, 1993.

[15] K. M. Siegel, "Far field scattering from bodies of revolution," *Appl. Sci. Res.*, vol. 7 (B), pp. 293-328, 1959.

[16] T. B. A. Senior, P. L. E. Uslenghi, "Further studies of back-scattering from a finite cone," *Radio Sci.*, vol. 8, pp. 247-249, 1973.

[17] W. D. Burnside, L. Peters, "Axial-radar cross section of finite cones by the equivalent-current concept with higher-order diffraction," *Radio Sci.*, vol. 7, pp. 943-948, 1972.

[18] D.-S. Wang, I. N. Medgyesi-Mitschang, "Electromagnetic scattering from finite circular and elliptic cones," *IEEE Trans. Antennas Propag.*, vol. 33, no. 5, pp. 488-497, May 1985.

[19] D. B. Kuryliak, Z. T. Nazarchuk, "The field of a radial electric dipole on the axis of a semi-infinite radially slotted cone", *Telecommunications and Radio Engineering*, vol. 61, no 10, pp. 861-874, 2004.

[20] D. B. Kuryliak, Z. T. Nazarchuk, "Excitation of axisymmetric electromagnetic oscillations in a system of coaxial finite and truncated cones with different flare angles", *Telecommunications and Radio Engineering*, vol. 63, no 1, pp. 15-31, 2005.

[21] R. D. Smedt, J. G. Van Bladel, "Field singularities at the tip of a metallic cone of arbitrary cross section," *IEEE Trans. Antennas Propag.*, vol. 34, pp. 865-870, July 1986.

[22] S. Marchetti, T. Rozzi, "Electric field behavior near metallic wedges," *IEEE Trans. Antennas Propag.*, vol. 38, no. 9, pp. 1333-1340, Sept. 1990.

[23] J. N. Sahalos, G. A. Thiele, "The eigenfunction solution for scattered fields and surface currents of a vertex," *IEEE Trans. Antennas Propag.*, Vol. AP-31, No.1, pp. 206-211, Jan. 1983.

[24] M. I. Kontorovich, N. N. Lebedev, "About one method for solving several problems of diffraction theory related objectives," *J. Techn. Physics*, vol. 8, no. 10-11, pp. 1192-1206, 1938 (in Russian).

[25] D. C. Pridmore-Brown, "The transition field on the surface of a slot-excited conical antenna," *IEEE Trans. Antennas Propag.*, vol. 21, no. 6, pp. 889-890, 1973.

[26] V. A. Doroshenko, V. G. Sologub, "On the structure of the field of a radial magnetic dipole scattered by a slotted conical surface," *Soviet J. Commun. Technol. Electronics*, vol. 32, no. 7, pp. 161-163, 1987.

[27] C.A. Balanis, *Advanced Engineering Electromagnetics*, New York, Wiley Publ., 1989.

[28] A. I. Nosich, "The method of analytical regularization in wave-scattering and eigenvalue problems: foundations and review of solutions," *IEEE Antennas Propag. Magazine*, vol. 41, no. 3, pp. 34-48, June 1999.

[29] Z. S. Agranovich, V. A. Marchenko, V. P. Shestopalov, "Diffraction of a plane electromagnetic wave from plane metallic lattices," *Soviet Technical Physics*, vol. 7, pp. 277-286, 1962.

[30] T.L. Zinenko, A.I. Nosich, Y. Okuno, "Plane wave scattering and absorption by resistive-strip and dielectric-strip periodic gratings", *IEEE Trans. Antennas Propag.*, vol. AP-46, no 10, pp. 1498-1505, 1998.

Elena K. Semenova (S'04-M'07) was born in Kharkiv, Ukraine, in 1977. She received the M.Sc. degree in applied mathematics from the Kharkiv National University in 2000 and the Ph.D. degree in radio physics from Kharkiv National University of Radio Electronics in 2005. Since 2004 she has been an assistant professor with the Mathematics Department of the latter university.

Her current research interests include analytical and numerical modelling of electromagnetic scattering with application to antennas. In 2003, she was a recipient of the travel grant of the Civilian R&D Foundation, USA for attending the IEEE Antennas and Propagation Symposium in Columbus, OH. In 2006, she received a travel grant of the IEEE Voluntary Contributions Fund of Region 8 for attending the International Conference on Transparent Optical Networks in Nottingham, UK. In 2004, she was awarded a Young Scientist Award of the International Conference on Mathematical Methods in Electromagnetic Theory held in Dnipropetrovsk, Ukraine.

Vladimir A. Doroshenko (M'04-SM'06) was born in Kharkiv, Ukraine, in 1954. He received the M.Sc. degree in mathematics from the Kharkiv National University in 1977, the Ph.D. degree in radio physics from the Institute of Radio Physics and Electronics of the National Academy of Sciences of Ukraine (IRE NASU) in 1989, and the D.Sc. degree in radio physics from the Kharkiv National University of Radio Electronics (KhNURE) in 2005. In 1977-1990, he was on research staff of IRE NASU as research engineer and then scientist. In 1990-1991, he worked as senior scientist with the Ukrainian Research Institute for Natural Gases, Kharkiv. In 1992-2006, he was with the Mathematics Department of KhNURE as lecturer and then associate professor (1993). In 1996-2004, he had been also part-time senior scientist of IRE NASU. Since 2006 he is professor and Dean of the School of Applied Mathematics and Management at KhNURE.

His current research interests include mathematical physics, electromagnetic theory, scattering and diffraction, integral transforms and equations, initial and time-harmonic boundary problems for the impedance, semitransparent and perfectly conducting 3D structure with emphasis of singular integral equations and analytical regularization.